PALEOCEANOGRAPHY, VOL. 12, NO. 1, PAGES 97-110, FEBRUARY 1997

Numerical modeling of late Glacial Laurentide advance of ice across Hudson Strait: Insights into terrestrial and marine geology, mass balance, and calving flux

W. T. Pfeffer,[1] M. Dyurgerov,[2] M. Kaplan,[1] J. Dwyer,[2,3] C. Sassolas, [2]
A. Jennings, [1] B. Raup, [1,4] and W. Manley [1]

Abstract. A time-dependent finite element model was used to reconstruct the advance of ice from a late Glacial dome on northern Quebec/Labrador across Hudson Strait to Meta Incognita Peninsula (Baffin Island) and subsequently to the 9.9-9.6 ka ^{14}C Gold Cove position on Hall Peninsula. Terrestrial geological and geophysical information from Quebec and Labrador was used to constrain initial and boundary conditions, and the model results are compared with terrestrial geological information from Baffin Island and considered in the context of the marine event DC-0 and the Younger Dryas cooling. We conclude that advance across Hudson Strait from Ungava Bay to Baffin Island is possible using realistic glacier physics under a variety of reasonable boundary conditions. Production of ice flux from a dome centered on northeastern Quebec and Labrador sufficient to deliver geologically inferred ice thickness at Gold Cove (Hall Peninsula) appears to require extensive penetration of sliding south from Ungava Bay. The discharge of ice into the ocean associated with advance and retreat across Hudson Strait does not peak at a time coincident with the start of the Younger Dryas and is less than minimum values proposed to influence North Atlantic thermohaline circulation; nevertheless, a significant fraction of freshwater input to the North Atlantic may have been provided abruptly and at a critical time by this event.

1. Introduction

The discharge of large quantities of glacier ice into the North Atlantic has been suggested as possibly forcing the cessation of North Atlantic Deep Water formation and consequently blocking the release of oceanic heat to the atmosphere in the North Atlantic region [*Broecker*, 1994]. The effect of freshwater and ice rafting on deep water formation and climate can be profound and rapid [*Rahmstorf*, 1995]. Episodic marine sediment layers found across the North Atlantic, termed "Heinrich events" [*Heinrich*, 1988], containing large clasts presumed to be transported by ice rafting, provide evidence of timing and areal extent of iceberg production and transport in the North Atlantic. Heinrich event H-0 in the North Atlantic and detrital carbonate event DC-0 in the Labrador Sea are broadly contemporaneous with Younger Dryas climatic cooling at 11.0-10.0 ka ^{14}C [*Andrews et al.*, 1995] (we correct ^{14}C dates for an assumed ocean reservoir effect by subtracting 450 years [*Bard et al.*, 1994]). While marine evidence is strong for ice-rafting events, the terrestrial source of icebergs is undetermined. Patterns of marine deposition in the northeast Atlantic and Labrador Sea strongly suggest that Heinrich events H-0, H-1, and H-2 originate from Hudson Strait [*Dowdeswell et al.*, 1995], and numerical models have successfully reproduced aspects of Heinrich events under the assumption that icebergs originate from Hudson Strait [*MacAyeal*, 1993]. Events H-1 and H-2 appear to be associated with flow along the Hudson Strait axis, but direct terrestrial evidence of glacier advance or retreat associated with calving events at these times is lacking. Terrestrial evidence on Baffin Island [*Kaufman et al.*, 1993; *Miller and Kaufman*, 1990; *Miller et al.*, 1988] and marine evidence from the Baffin Shelf [*Andrews et al.*, 1995] indicate that DC-0/H-0 is associated with flow from the Ungava platform north-northeast across Hudson Strait to eastern Meta Incognita Peninsula.

[1]Institute of Arctic and Alpine Research and Department of Geological Sciences, University of Colorado, Boulder.
[2]Institute of Arctic and Alpine Research, University of Colorado, Boulder.
[3]Now at Department of Mechanical Engineering, University of New Hampshire, Durham.
[4]Now at U.S. Geological Survey, Flagstaff, Arizona.

Paper number 96PA03065.
0883-8305/97/96PA-03065$12.00

Miller and Kaufman [1990] and *Andrews et al.* [1990] considered the possibility that glacier advance and retreat in the Hudson Strait region might have triggered the Younger Dryas, based on the spatial and temporal structure of advance of ice across Hudson Strait from northern Quebec and Labrador onto southern Baffin Island. Advance was initiated as early as ~11.0 ka ^{14}C (contemporaneous with the onset of DC-0/H-0 [*Andrews et al.*, 1995]) and culminated in two maxima at ~9.9 (Gold Cove) and ~8.7 (Noble Inlet) ka $^{14}C \pm 100$ years [*Kaufman et al.*, 1993; *Manley*, 1995]. The Gold Cove advance reached its maximum extent on southeastern Hall Peninsula after a rapid (~300 – 400 year) advance across Frobisher Bay. The advance may have started from the Ungava platform or, alternatively, from a stable intermediate position at Meta Incognita Peninsula, Resolution Island, and the sill dividing the Eastern and Hatton Basins (referred to here as MIRI; Figure 1). Following retreat from Gold Cove, Hudson Strait became partially ice free before the second advance to Noble Inlet, but we do not address the Noble Inlet advance here.

We present a synthesis of terrestrial geological evidence and modeling results from Younger Dryas/DC-0 time and consider whether the pattern of advance, retreat, and calving inferred from the terrestrial and marine geologic records up to the time of recession from the Gold Cove maximum can be reproduced in a numerical model which allows for fairly realistic treatment of ice flow dynamics, basal sliding, flotation and calving, terrestrial topography, ice geometry, and mass balance. We also discuss how modeled discharge fluxes relate to timing and location of sediment discharge inferred from marine event DC-0 and to meltwater fluxes required to affect North Atlantic circulation.

2. Model Description

A numerical model of glacier dynamics with ice-ocean interaction requires simulation of nonlinear creeping flow of ice under gravitational driving forces, basal sliding of ice over bedrock, addition and subtraction of ice by accumulation and ablation, flotation of ice in seawater, and calving of icebergs. Isostatic depression is not considered here because the model simulation time is short (3 kyr total) relative to rates of isostatic adjustment. Sea level is set at +40 m above present sea level throughout the simulation to represent average isostatic depression for the region.

2.1. Ice Motion

Calculations are done with a two-dimensional ("map plane") finite element model based on an original version developed by *Fastook and Chapman* [1989] and modified by us to include longitudinal stress coupling, floating ice, and iceberg calving. Bedrock and ice surface height, ice surface gradient, and column-integrated flux are given at each nodal point in a two-dimensional map space. Numerical solutions in the original (unmodified) model are obtained for the time-varying ice height on realistic bedrock terrain. Ice motion follows conventional formulations such as *Paterson* [1994],

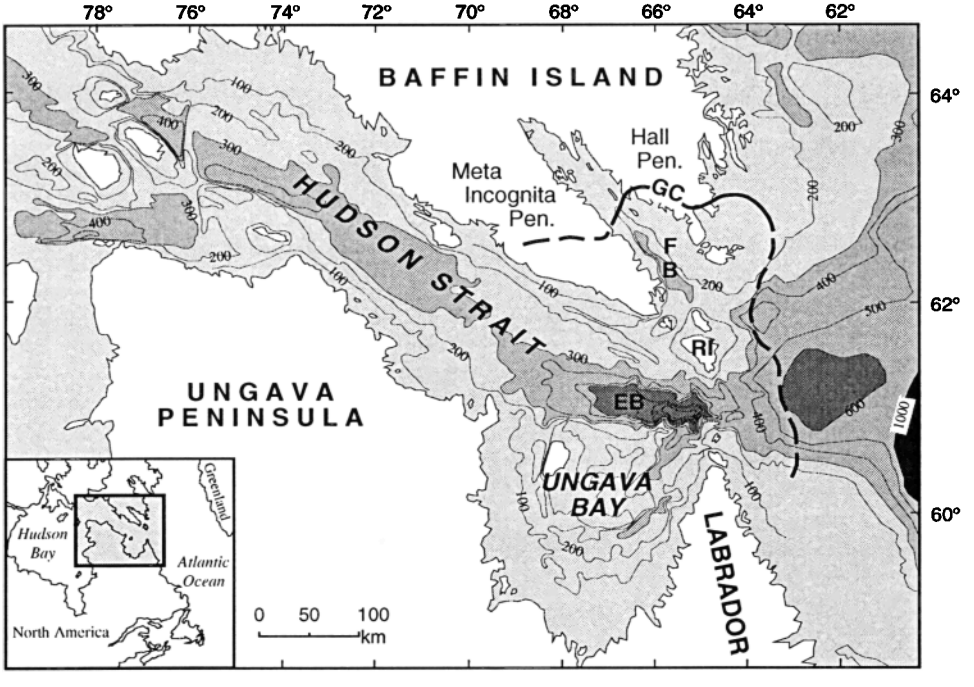

Figure 1. Bathymetry of Hudson Strait. EB marks Eastern Basin, RI marks Resolution Island, FB marks Frobisher Bay, and GC marks Gold Cove maximum position determined from terrestrial and marine geology.

with the difference that the flow parameter A here follows the form $\dot{\epsilon} = (\tau/A)^n$, for which A has dimensions $[ML^{-1}T^{(1/n-2)}]$, in contrast to a common alternative formulation, which follows the form $\dot{\epsilon} = A\tau^n$ and for which A has dimensions of $[M^{-n}L^nT^{(2n-1)}]$. Total velocity U consists of internal deformation

$$U_f = \frac{2}{n+2}\left(\frac{\tau_b}{A}\right)^n H \tag{1}$$

and basal sliding

$$U_s = \left(\frac{\tau_b}{B}\right)^m \tag{2}$$

where U_f is the column-averaged internal deformation velocity, U_s is sliding velocity, and H is ice thickness. The basal shear stress $\tau_b = \rho g H(\sin\alpha)$, where ρ is ice density, g is gravitational acceleration, and α is surface slope. The total velocity is $U = \phi U_s + (1-\phi)U_f$, where ϕ is a parameter controlling the relative contributions of flow and sliding and is set or varied in accordance with observed terrestrial and marine geology. Parameters n, m, A, and B are set to $n = 3$, $m = 2$, $A = 3.0$ bars $\mathrm{yr}^{(1/3)}$ and $B = 0.01$ bars $(\mathrm{m/yr})^{(-1/2)}$. Experiments in which the flow parameter A was varied within reasonable limits were found to have only minor effects on ice velocity and speed of advance, and variations in the basal sliding parameter B within reasonable limits were tried and found to have less effect on model behavior than the location of sliding. In the absence of information to modify the magnitudes of A and B and in the interests of reducing the number of free parameters, we fix A and B at the values given above and rely on geological information to constrain the location of sliding, as described below.

Integrated column-averaged velocities provide the ice flux arising from local driving stress, determined as a function of ice thickness H and surface elevation gradient ∇h and local longitudinal velocity gradients. The fluxes are combined, and individual element flux $\vec{Q}$ is determined for each quadrilateral element based on the gradient of surface elevation

$$\vec{Q}(x,y,t) = \vec{U}H = -k(x,y,t)\vec{\nabla}h(x,y,t) \tag{3}$$

where $\vec{U}$ is the vertically averaged total ice velocity and $k(x,y,t)$ is a nonlinear coefficient derived from integration over thickness H of the expressions for sliding and deformational velocities. Coordinates x and y are orthogonal horizontal spatial axes, and t is time. A continuity equation is solved at each time step to determine the new ice surface elevation created by processes of interelement flow and surface mass balance

$$\frac{\partial h}{\partial t} = \dot{a} - \nabla Q \tag{4}$$

where $\dot{a}$ is the spatially and temporally variable mass balance.

Boundary conditions include the location of basal sliding, calving on floating marine margins, and surface mass balance. In contrast to models in which basal sliding is determined internally by the action of stress equilibrium and thermal and hydrological processes, sliding is controlled here externally as a function of location and time by adjusting the parameter ϕ.

2.2. Modifications to the Original Model

The original numerical model of *Fastook and Chapman* [1989] determines velocity strictly in terms of local surface slope and thickness as given in equations (1) and (2). We apply a modification which allows longitudinal (along-flow) velocity gradients to influence local stresses and velocities, following *Budd* [1970].

The basal shear stress τ_b is defined as

$$\tau_b = \rho g H|\nabla h| + 2G \tag{5}$$

where

$$G = H\frac{\partial \overline{\tau_{xx}}}{\partial x} \tag{6}$$

where the overbar indicates averaging of the deviatoric stress τ_{xx} over the ice thickness. In terms of Glen's law,

$$\overline{\tau_{xx}} = A\left(\frac{\partial U}{\partial x}\right)^{\frac{1}{n}} \tag{7}$$

where, again, U is the vertically averaged total velocity. The basal shear stress (equation (5)) is now written as

$$\tau_b = \rho g H|\nabla h| + 2AH\frac{\partial}{\partial x}\left(\frac{\partial U}{\partial x}\right)^{\frac{1}{n}} \tag{8}$$

The expressions for deformational and sliding velocity become

$$\begin{aligned}\vec{U}_f &= \frac{2}{n+2}\left(\frac{\tau_b}{A}\right)^n H\left(\frac{-\nabla h}{|\nabla h|}\right)\\ &= \frac{2H}{(n+2)A^n}\left[\rho g H|\nabla h| + 2AH\frac{\partial}{\partial x}\left(\frac{\partial U}{\partial x}\right)^{\frac{1}{n}}\right]\left(\frac{-\nabla h}{|\nabla h|}\right)\end{aligned} \tag{9}$$

$$\vec{U}_s = B^{-m}\left[\rho g H|\nabla h| + 2AH\frac{\partial}{\partial x}\left(\frac{\partial U}{\partial x}\right)^{\frac{1}{n}}\right]^m\left(\frac{-\nabla h}{|\nabla h|}\right) \tag{10}$$

The modified expression for $k(x,y)$ is

$$\begin{aligned}k(x,y) &= \frac{H}{|\nabla H|}\left[\phi U_s + (1-\phi)U_f\right]\\ &= \frac{H}{|\nabla H|}\left[\phi B^{-m}\tau_b^n + (1-\phi)\frac{2H}{A^n(n+2)}\tau_b^n\right]\end{aligned} \tag{11}$$

Singularities may occur in terms containing

$$\partial/\partial x\,(\partial U/\partial x)^{1/n}$$

(equations (8), (9), and (10)). This is implemented in the numerical solution in the form

$$\frac{\partial}{\partial x}\left(\frac{\partial U}{\partial x}\right)^{\frac{1}{n}} = \frac{1}{n}\frac{\partial^2 U}{\partial x^2}\left(\frac{\partial U}{\partial x}\right)^{\frac{1-n}{n}}. \qquad (12)$$

If the first derivative term approaches zero it is assumed that velocity gradients are sufficiently small that the entire G term (the second term on the right-hand side of equation (8)) can be set to zero, and the singularity is avoided.

Once the inclusion of longitudinal velocity gradients is achieved, the length over which the gradients apply must be decided. This problem has been discussed by *Budd* [1970] and also by *Kamb and Echelmeyer* [1986]; in our model the averaging length is an integer number of neighboring elements and is controlled as an external parameter. For the present application it is set to the nearest neighbors (the derivative extends to the far boundaries of the immediate neighbors of the current element) and is held fixed. The details of the numerical averaging are given by *Raup* [1995].

In addition to the inclusion of longitudinal gradients, major modifications were made to the original model in the inclusion of floating ice and iceberg calving. Floating ice is handled simply by determining, for water-covered locations, where ice is thick enough in the current time step to ground in the water depth at that location. If the ice is not thick enough to ground, then the ice surface and base elevations are set at the appropriate levels for flotation, given the current ice thickness. Mass continuity is maintained as on land and causes changes in the thickness of floating ice over time. Ice shelf spreading is not implemented in the present version; flow and thinning of floating ice is driven by surface slope, as on land, but with no basal coupling. This approximation of floating ice dynamics allows ice to thin and flatten as it leaves the grounding line, but continued spreading under zero surface slope does not occur. Zero-slope ice shelf spreading is much smaller in magnitude than slope-driven thinning, and simple sensitivity tests showed that it can be ignored in the present application where the lifetime of floating ice is short.

Iceberg calving is a complex and poorly understood process and is in any case difficult to represent realistically in a continuum model with large elements relative to potential iceberg size. Our model representation of calving employed here is based on work of *Reeh* [1968] and *Fastook and Schmidt* [1982]. A review of work specifically on calving mechanics, including our own work related to this model, is given by *Sassolas et al.* [1996]. We include calving as an ablation term acting at elements along the perimeter of floating ice margins. Calving flux is calculated as a product of iceberg size, estimated by the probable position of fracture at one ice thickness behind a floating ice cliff [*Reeh*, 1968], and time-to-breakoff, determined by integrating a theoretically derived depth-dependent crack propagation rate over the depth of the floating ice margin. We obtained crack propagation rates as a function of depth from *Fastook and Schmidt* [1982]. Their results were synthesized to obtain the following relation between time-to-breakoff (t_c, years) and floating ice thickness (h, meters):

$$t_c = 3.33(1.0 - e^{-0.0031h})$$

The calving flux (dimensions of $[L^3T^{-1}]$) for one element on the floating perimeter is then

$$q_c = \frac{d_c h e_w}{t_c}$$

where d_c is the crack distance behind the floating ice edge and e_w is the element width. The calving speed (dimensions of $[LT^{-1}]$) is

$$C = \frac{Q_c}{{e_w}^2}$$

Calving speed C is treated as a mass balance term in the calving element. Calving can eliminate perimeter elements altogether, allowing for retreat of a floating margin due to calving. The calving flux calculation as described appears to be very conservative (low flux for given thickness), but no appropriate observational data exist for comparison.

2.3. Mass Balance

Mass balance plays a key role in the reproduction of the dynamics of advance and retreat at DC-0/Younger Dryas time. Our modeling strategy is to fix as many parameters as possible and vary the remaining ones within limits constrained by observation. The model mass balance must be allowed to vary over time to reproduce the observations; this is not surprising in view of the rapidly varying climatic conditions at the Younger Dryas/Preboreal transition. We took the timing and magnitude of shifts in precipitation and temperature from the central Greenland GISP2 ice core paleoclimate record [*Alley et al.*, 1993] and applied them to an elevation distribution for Quebec/Labrador (Figure 2a) constructed from observations for the modern Devon ice cap [*International Association of Hydrological Sciences (IAHS)*, 1988, 1993] and central west Greenland [*Ohmura*, 1993]. Equilibrium line elevation (ELA) sensitivity to summer temperature was represented by a linear relationship between annual (T_{ann}) and summer (T_{JJA}) temperatures at Resolution weather station and between T_{JJA} and present-day ELA (1961-1990 time period) for the Devon ice cap [*IAHS*, 1988, 1993]. Past ELA positions were then determined in terms of past T_{ann}. Annual ice ablation (M) at the Quebec/Labrador ice dome margin is calculated using an empirical formula [*Krenke and Chodakov*, 1966]:

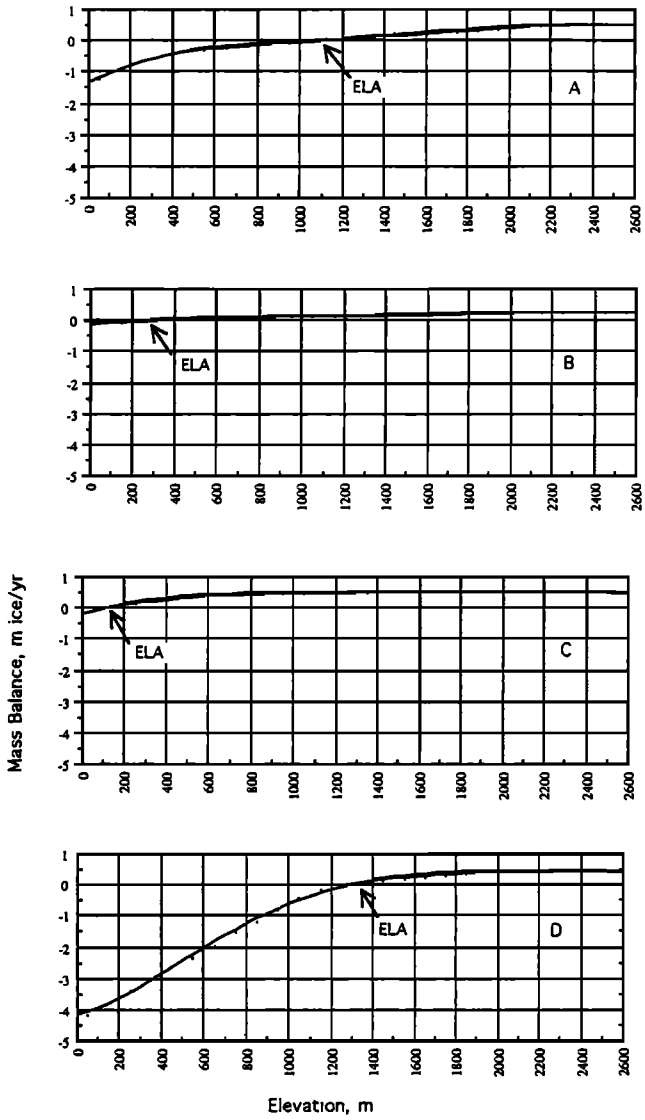

Figure 2. Mass balance distributions used in model: (a) synthesized mass balance profiles from modern Devon Ice Cap and west Greenland data; (b) Younger Dryas mass balance; (c) transitional I mass balance (Gold Cove advance); and (d) transitional II mass balance (recession from Gold Cove)

$$M = (T_{JJA} + 9.5)^3$$

where T_{JJA} has units of °C and M is melt in millimeters water equivalent. Mass balance parameters for the sequence of changes during and following the Younger Dryas are summarized in Table 1.

Mass balance was simulated in three phases: a cold, dry Younger Dryas condition; a high accumulation, low ELA condition (transitional I) following the Younger Dryas and driving the Gold Cove advance; and a high accumulation, high ELA condition (transitional II) driving recession from Gold Cove. Mass balance for the Younger Dryas was constructed by shifting the modern curve (Figure 2a) to a cold, low accumulation, low ELA environment (Figure 2b). Accumulation was increased by 100% at the Younger Dryas termination to drive advance to Gold Cove (transitional I, Figure 2c). The accumulation and temperature are increased at all elevations, with the effect of accumulation dominating temperature at low elevations, resulting in a depressed ELA despite warming temperatures and advection of warmer ice at Gold Cove time. Recession from Gold Cove is driven by increased ablation and elevated ELA, which are consequences of warming of +7°C (from −25°C to −18°C [*Alley et al.*, 1993]) over the Younger Dryas/Holocene transition (transitional II, Figure 2d).

2.4. Initial Model Inputs

The simulation region extends from the Gulf of St. Lawrence to the north shore of Cumberland Sound (Baffin Island) and from Hudson Bay to the Labrador Sea. Bedrock topography at 9216 nodes covering the model region is interpolated from the 5-min ETOPO5 digital terrain model [*National Oceanic and Atmospheric Administration (NOAA)*, 1988]. The initial ice sheet was "grown" by specifying a positive mass balance over the center of the dome. During buildup, no basal sliding is allowed. After approximately 1000 years of simulation, the mass balance is switched to the Younger Dryas rule (Figure 2b), and the ice dome is allowed to stabilize over another ~ 300 years. The resulting quasi steady state ice dome has a maximum central thickness (2200 m) and location consistent with *Peltier's* [1994]

Table 1. Reconstructed Climatic and Mass Balance Variables for Quebec/Labrador Ice Sheet

Glacial Stages	Annual Accumulation[a]	Difference in T_{ann}[b]	Summer Temperature, °C	Annual Ablation, m ice	Annual Mass Balance, m ice	Equilibrium Line Elevation, m above sea level
Younger Dryas	50	-10	-4.8	-0.15	+0.5	300
Transition I	100	-8	-4.0	-0.25	+0.7	120
Transition II	100	-2	+0.5	-4.20	0.0	1300

[a]% Change From Present
[b](Present - Reconstructed), °C

calculations based on isostatic rebound and *Kleman et al.*'s [1994] analysis of landforms in Quebec/Labrador. The ice thickness is a maximum value compatible with Peltier (although *Edwards* [1995] suggests that Peltier's net ice volume may be an underestimate) and is centered slightly to the northeast of Peltier's placement of the maximum ice thickness. Hudson Strait is initially ice free. While no definitive evidence exists which constrains ice conditions in Hudson Strait immediately prior to DC-0, marine conditions at the nearby Resolution Basin and SE Baffin Shelf indicate relatively warm and possibly seasonally ice-free conditions [*Andrews et al.*, 1995]. *Kleman et al.* [1994] interpreted the set of convergent flow indicators south of Ungava Bay to be a pre-Late Wisconsin relict landscape preserved by frozen, no-slip bed conditions at Late Wisconsin time. In accordance with this, we do not allow sliding anywhere above modern sea level south of Hudson Strait. At the start of the simulation, sliding is allowed wherever ice is present in Ungava Bay, Hudson Strait, and all regions to the north of Hudson Strait at model time equal to 0; this event defines the onset of advance.

Kleman et al.'s [1994] interpretation of superimposed landforms on Quebec/Labrador imposes a constraint on basal boundary conditions which is held fixed throughout these model experiments. We will return to this constraint in the discussion and consider its plausibility in light of the results.

3. Model Results

Figures 3-5 show representative surface elevation maps and cross sections of an ice dome originating from Quebec/Labrador at stages from the initial configuration to recession following the Gold Cove maximum. Model simulations were made in three phases: (1) advance across Hudson Strait to a stable position on Meta Incognita Peninsula and Resolution Island (MIRI), coincident with the start of DC-0/Younger Dryas time; (2) advance from MIRI to Hall Peninsula coincident with the Gold Cove advance; and (3) rapid retreat from Hall Peninsula to MIRI and finally southern Hudson Strait. Model result times correspond to calendar year intervals, and where possible, we identify equivalent times in the ^{14}C chronology in which the terrestrial record is set. The initiation of the first advance across Hudson Strait corresponds in time to the onset of the Younger Dryas, at $\sim 11 \pm 0.1$ ka ^{14}C.

3.1. Advance Across Hudson Strait

Given the fixed spatial pattern of sliding, successful advance of ice across Hudson Strait from an initial position on Quebec/Labrador requires an initial maximum ice thickness of at least 2000 m (Figure 3). Initial ice heights less than this resulted in drawdown of the central portion of the dome and insufficient upstream ice flux to overcome calving in the Eastern Basin. Using a 2200-m initial ice height, advance to MIRI occurs in approximately 300-400 years, with the highest discharge fluxes during this phase (0.0025 Sverdrup (Sv)) occurring as ice crosses the deep Eastern Basin. After reaching MIRI, the terminus stabilizes in shallow water and maintains equilibrium at this position (with consequent changes in thickness and discharge) over a moderate range of reasonable mass balance values. Figure 4 shows the ice configuration at the stable MIRI position. Given the constraints of ice thickness, location of sliding, and the simplicity of our calving rule, the advance to MIRI is a robust result and confirms the plausibility of successful advance of ice across Hudson Strait under reasonable conditions.

3.2. Gold Cove Advance

With the distribution of sliding held fixed, we attempted to find realistic conditions of mass balance and calving which allow rapid advance beyond MIRI to Hall Peninsula ($\sim$400 years or less), ice thicknesses at Hall Peninsula consistent with observations [*Kaufman et al.*, 1993] of coverage of summits (+400 m above sea level (asl)), and rapid retreat from Hall Peninsula to MIRI (400 years or less). The northern margin of the advance, extended at the MIRI position, is isolated from the main dome, and even with longitudinal coupling, changes in mass balance at the main dome are found to have no immediate or short-term effect on the MIRI margin. We used an abrupt increase in precipitation preceding a rise in ELA at the termination of the Younger Dryas to drive the onset of the Gold Cove advance at $\sim$10.2 ka ^{14}C. Rapid initial advance is driven by increased accumulation in the extended lobe over Hudson Strait. Mass balance as given in Figure 2c provides sufficient accumulation to produce rapid advance of ice past the stable MIRI position to Gold Cove but is at the upper limit of reasonable accumulation rates and only delivers ice of $\sim$ 100 m thickness to Hall Peninsula. Actual ice thickness on Hall Peninsula during the Gold Cove advance is constrained by bedrock striations at 370 m asl on Loks Land (easternmost Hall Peninsula) [*Kaufman et al.*, 1993], so the model clearly underestimates ice thickness at Hall Peninsula. The shape of the advanced lobe on Meta Incognita and Hall Peninsulas (Figure 5) matches remarkably well the spatial pattern inferred from the terrestrial geology (compare our Figure 1 with Figure 1 of *Kaufman et al.* [1993]). Further experiments with greater (unrealistic) accumulation rates failed to produce substantially thicker ice at Hall Peninsula.

The timing of the changes to a higher accumulation rate (Figure 2c) controls the timing of advance to Gold Cove. The time at which the increase in accumulation is applied is determined here by the model response and acts as a tuning parameter. The mass balance shift for Gold Cove is supported by GISP2 data only for a very brief period ($\sim 5 - 25$ years) in central Greenland but is maintained here during the duration of the Gold Cove advance. This is an unrealistically long time in

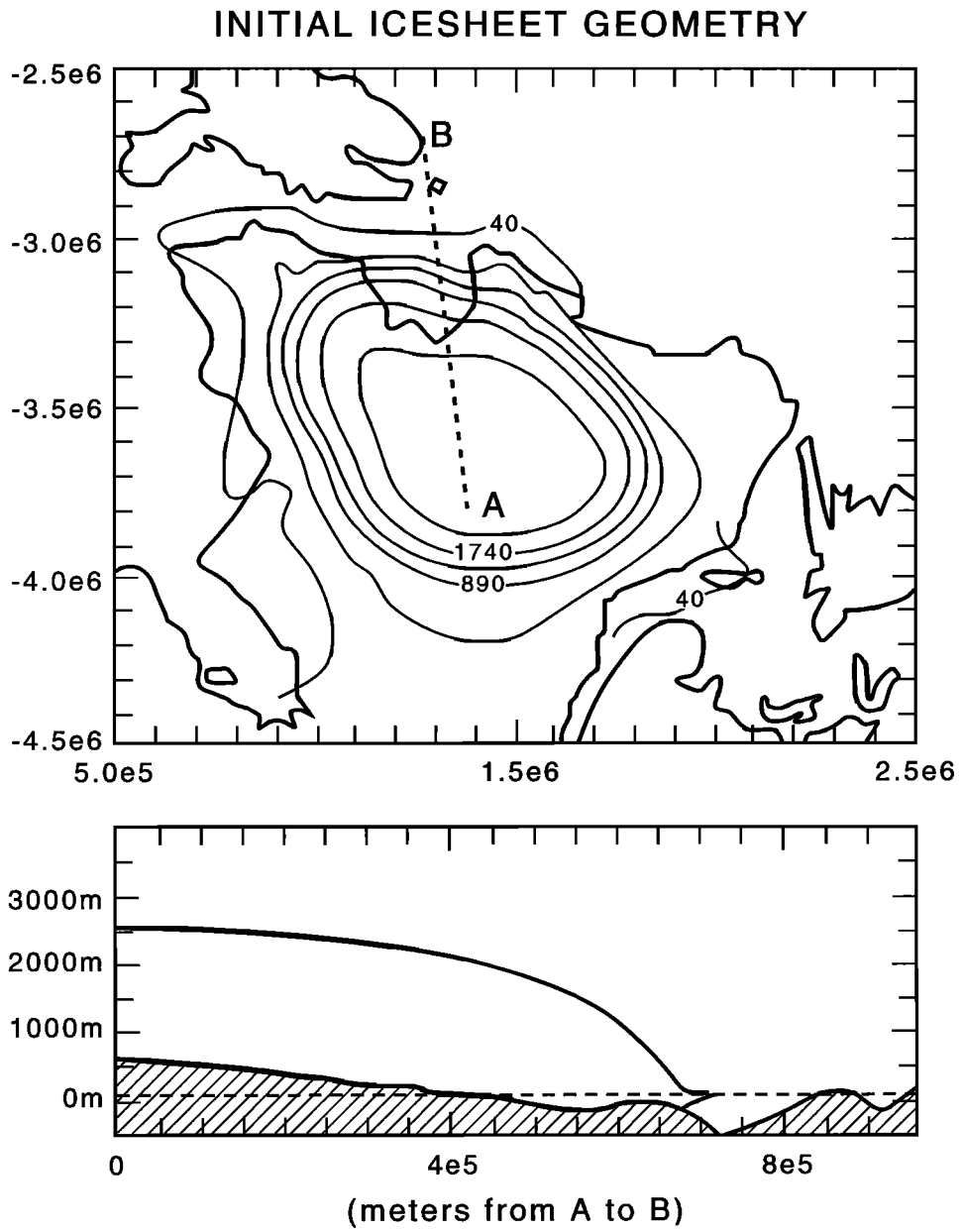

Figure 3. Initial ice geometry on Quebec/Labrador. Map region includes northern Quebec, Hudson Strait, and southern Baffin Island. Axes in upper panel show Universal Transverse Mercator (UTM) coordinates. Lower panel shows elevation transect from A to B indicated in upper panel.

the context of the GISP2 record but is necessary in context of the model boundary conditions to force the advance. *Kaufman et al.* [1993] show ^{14}C dates which constrain the occupation of Frobisher Bay by ice to ~ 100 – 500 years. Our model results are consistent with this constraint.

3.3. Recession

Changing conditions at the end of the Younger Dryas are simulated by increased rates of accumulation and ablation and a rise in ELA (Figure 2d). Rapid retreat from Gold Cove to MIRI, and beyond to Ungava Bay, occurs primarily as a consequence of rising ELA and to a lesser extent as a consequence of upstream thinning in response to advance. In addition to calving, thinning lowers a large fraction of the surface of the extended lobe below the ELA and abruptly exposes most or all of the lobe to ablation. Ice grounded in the deep Eastern Basin of Hudson Strait early in the cross-strait advance (~ 11.0 ka ^{14}C) becomes ungrounded following the Gold Cove maximum, whereupon rapid thinning and flotation exposes the extended lobe to greater rates

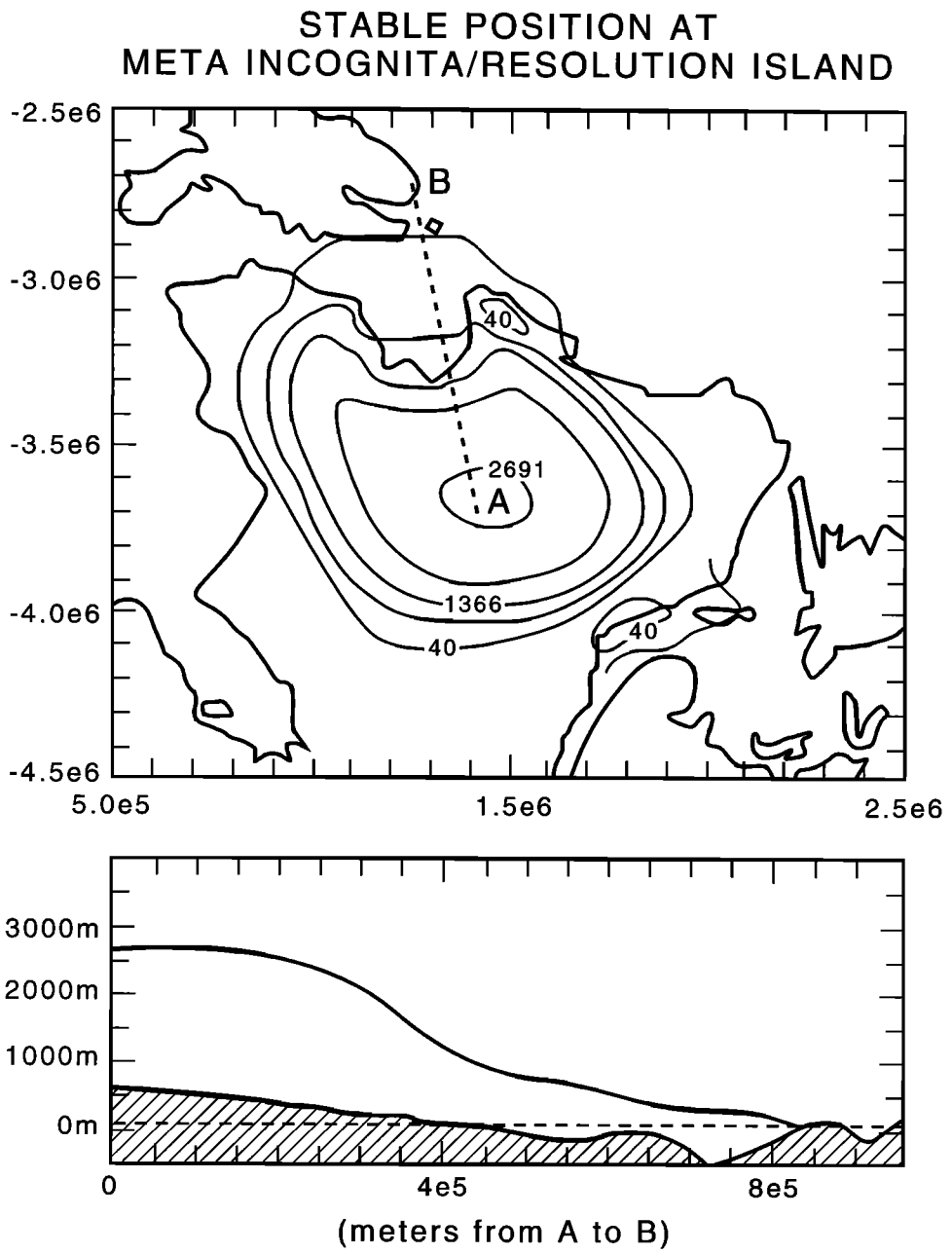

Figure 4. Modeled stable position at Meta Incognita Peninsula and Resolution Island (MIRI) at DC-0 time.

of melt and calving. The marine sediment signature in the Eastern Basin might be expected to be infilling of subglacial sediment older than ~ 9.5 ka ^{14}C, overlain by a brief layer of ice-rafted debris, with ice-free marine sediment immediately after.

3.4. Calving and Runoff Discharge Flux

Total ice discharge (sum of calving plus runoff from ice grounded below sea level) rates are shown in Figure 6 for the entire model sequence from the initial start-up time (~11.0 ka ^{14}C at start of DC-0) to nearly ice-free conditions following retreat from the Gold Cove maximum position. The highest discharge fluxes during advance to Gold Cove (0.0025 Sv) occur during the first 200 years of the simulation as ice crosses the deep Eastern Basin. The dramatic rise in discharge at the start of retreat from Gold Cove is due to an increase in runoff and is caused by the change from the transitional I mass balance to transitional II when the ELA rises from 320 to 1300 m.

Some experiments were made with a variable calving flux. Calving flux sensitivity was made a parameter

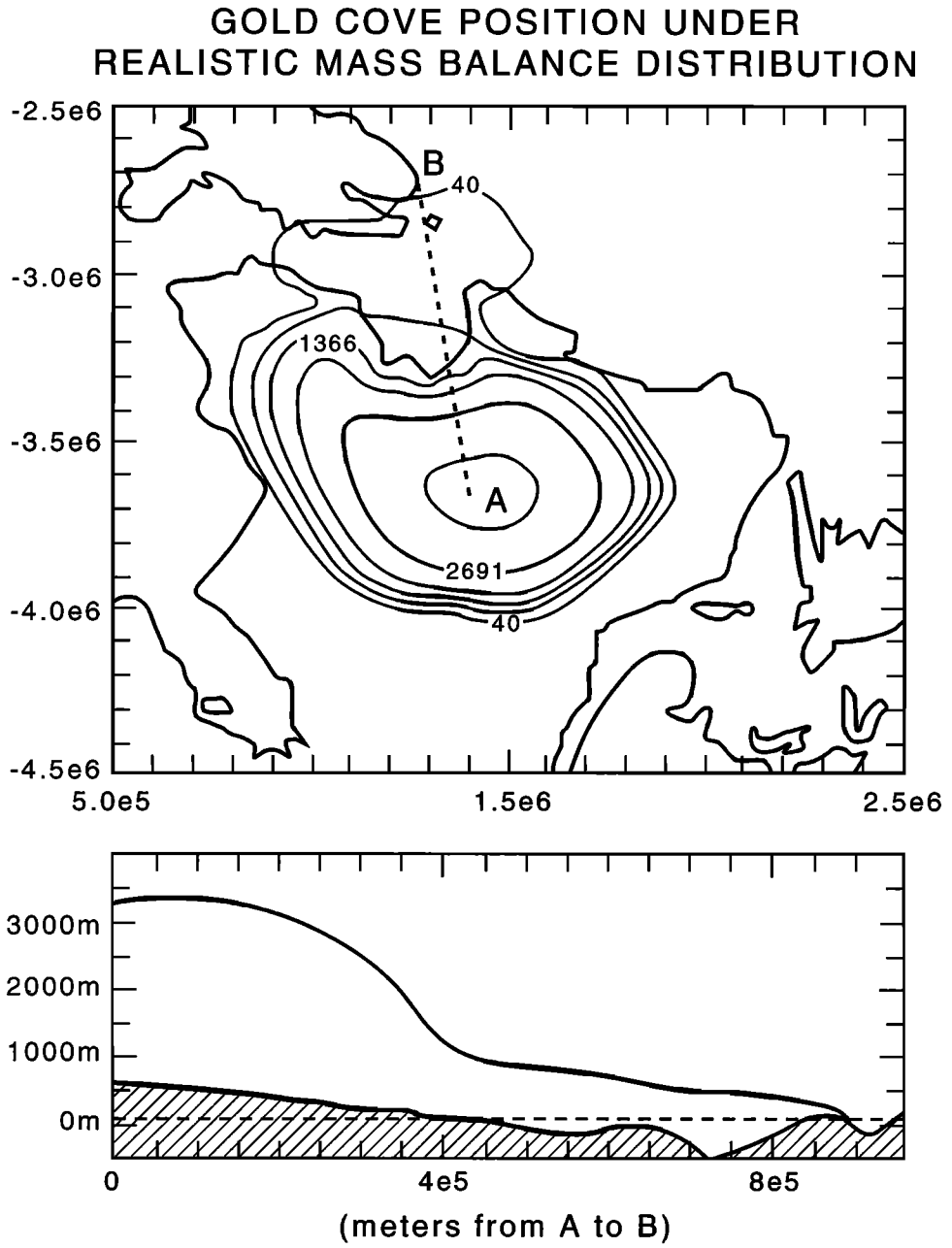

Figure 5. Modeled Gold Cove maximum extent corresponding to geological interpretation at 9.9 ka ^{14}C. Compare position shown in Figure 1.

and was adjusted to see if conditions could be obtained which would produce discharges of calved ice only which agree more closely with values inferred to affect North Atlantic thermohaline circulation. When calving flux was increased by a factor of 10 for a given ice thickness, calving discharge as great as 0.011 Sv developed during advance as the ice margin left the Ungava platform, but ice failed to cross Hudson Strait. The large calving rates are greater than can be supplied by ice flow from the south under the constraint imposed by the location of sliding. We rejected the higher calving flux (and consequent failure to cross the Strait) as being in conflict with the terrestrial geological observations on Meta Incognita and Hall Peninsulas, which indicates clearly the successful advance of ice onto Baffin Island. We regard the terrestrial geological interpretation on southern Baffin Island as more solidly established than the constraints placed on basal sliding in Labrador. The calculated discharge flux is a conservative estimate of discharge since our calving rule is conservative: A more highly reactive calving rule acts to increase the calving speed. While the high-rate calving flux (10 times normal) prevents ice from crossing Hudson Strait, it would be possible to optimize the calving rule to achieve the

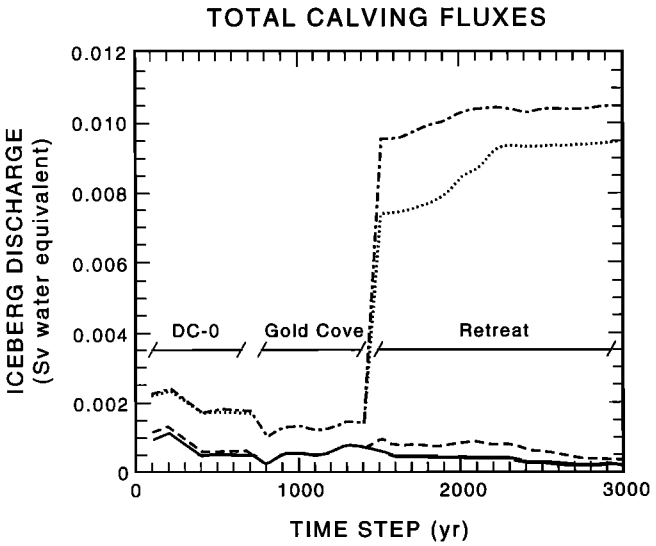

Figure 6. Modeled calving flux. Solid line denotes iceberg calving discharge only. Dashed line denotes icebergs plus runoff from calving elements only. Dotted line denotes icebergs plus runoff from all floating ice. Dashed-dotted line denotes icebergs plus runoff from all marine-grounded ice.

highest calving rate while allowing successful advance across the Strait. However, the same net volume of marine-grounded ice north of the Ungava platform is subject to loss during recession in any case.

Simple calculations of ice volume and flux provide constraints on calving flux from the Quebec/Labrador ice dome. Approximately 8×10^{13} m^3 of ice in our model simulation is grounded below sea level in Hudson Strait at the MIRI position. If a mechanism for sufficiently rapid removal of ice were present, this volume of ice would provide a flux to the ocean of 0.06 Sv (*Rahmstorf's* [1995] estimate of the flux required to shut down North Atlantic thermohaline circulation) for 42 years. A flux of 0.015 Sv (Rahmstorf's estimate of the flux required to shut down Labrador Sea only) could be sustained for 170 years. Rahmstorf's model requires freshwater input times over ~1000 years, however, and a flux of this magnitude cannot be obtained from the marine-based lobe alone for sufficient lengths of time, regardless of calving dynamics. *Manabe and Stouffer* [1995] simulate pulses of meltwater input over 10-year intervals but require much larger fluxes (~1 Sv) to affect thermohaline circulation. Without a closer dynamic connection between ice on Labrador and marine-grounded ice in Hudson Strait (again, the consequence of the limitation of sliding under the main dome), the marine-grounded ice already in place at the onset of recession is the only ice available for rapid evacuation by calving.

Miller and Kaufman's [1990] estimate of calving flux ranged from 300 to 2400 km^3 yr^{-1} (0.01 to 0.08 Sv), assuming an ice cross-sectional area of ~300 km^2 at the mouth of Hudson Strait and downstrait ice velocity ranging from 1 to 8 km yr^{-1}. These estimates are far in excess of our calculations of ~0.002 Sv for advance from Ungava to MIRI. Miller and Kaufman's estimates were based on the assumption that upstream ice flux must support large calving fluxes to the Labrador Sea from Hudson Strait simultaneously with advance to Gold Cove and that the magnitude of calving can be estimated from the velocities of large modern ice streams. Our model results, however, show that the MIRI position is relatively stable and resistant to calving and that it is evidently not necessary that cross-strait flow satisfy the additional demands of large calving fluxes to maintain a terminus position at or beyond Meta Incognita Peninsula.

In calculating their calving flux, *Miller and Kaufman* [1990] invoke much thicker ice than we calculate and also use a range of velocities greater than those we calculate. While we believe our ice thickness to be somewhat too small (based on the poor match of ice thickness at Gold Cove), Miller and Kaufman's cross-sectional area and maximum velocity appear to be much too large. Their maximum flux (2400 km^3 yr^{-1}) would supply the ice required to occupy the Gold Cove position (as calculated by our simulation) from the Ungava platform in only 42 years. We can allow very conservatively for our underestimation of volume by doubling the ice volume required and allowing 84 years for the Gold Cove advance at 2400 km^3 yr^{-1}. Further ice flux after the Gold Cove position is attained would have to be accommodated by nearly downstrait flow, or else the advance would continue past the Gold Cove position. A downstrait flux of 2400 km^3 yr^{-1} at the mouth of Hudson Strait, continued for a length of time compatible with *Rahmstorf's* [1995] requirements, would probably leave strong evidence of down-strait flow, but no clear evidence exists of this at DC-0 time from Meta Incognita Peninsula, or from Resolution, Button, or Killineck Islands [*Miller et al.*, 1988; *Stravers et al.*, 1992; *Manley et al.*, 1993; *Lauriol and Grey*, 1987]. Alternatively, without regard for the cross-strait advances, the Quebec/Labrador dome (8.1×10^{15} m^3 water equivalent) could not sustain such large discharge fluxes for a long period of time. At 2400 km^3 yr^{-1}, the entire dome volume would be consumed in less than 4000 years by calving alone, with no allowance for the Gold Cove or Noble Inlet advances. We contend that from DC-0 through final deglaciation following the Noble Inlet advance, the loss of the Quebec/Labrador dome generated large meltwater inputs to the North Atlantic but not predominantly as iceberg discharge through Hudson Strait and not at fluxes as large as 0.06 Sv at DC-0 time.

Discharge of ice and meltwater from Hudson Strait during advance and recession of the Quebec/Labrador dome could have been substantially amplified by interaction with ice in western Hudson Strait or ice surrounding the Laurentide core in and around Hudson Bay. Reasoning by analogy with the Quebec/Labrador

advance at DC-0 time, and with flood drainage through the York canyons (Meta Incognita Peninsula) at Noble Inlet time ($\sim 8.9 - 8.4$ ka ^{14}C), *Johnson and Lauritzen* [1995] proposed that an ice dam blocking Hudson Strait at 116 ka (isotopic stage 5e-5d) was breached at the York canyons and that a large (6×10^5 km^3) lake impounded behind the dam drained, initiating surges of ice flowing into the lake. The proposed event would have produced a large influx of fresh water and ice to the north Atlantic: The volume of the proposed lake alone would produce a sea level rise of 1 m, while the observed sea level rise at 116 ka inferred by the authors was $\sim 5 - 10$ m.

The evidence as given by *Johnson and Lauritzen* [1995] supports a climatic and sea level event near 116 ka. However, while flooding through the York canyons is well established for Noble Inlet time [*Manley*, 1995; *Blake*, 1966], there is no definite evidence that drainage through the York canyons occurred prior to this time . Furthermore, the difference between calculated lake volume and inferred sea level rise ($\sim 4-9$ m sea level equivalent) would be accounted for by $\sim 2.6 - 6 \times 10^6$ km^3 of ice calved into the draining lake and exiting through the York canyons. Modern-day observation of iceberg entrapment in fjords strongly suggests that such a volume of icebergs would have a very difficult time passing through the York canyons, which are typically 1 km or less in width. Additionally, drainage would lower the level of an impounded lake only to the lowest sill depth (~ 290 m) of the York canyons. We suggest that any jökulhlaup event containing significant ice must have drained by removal of the main blockage of ice in eastern Hudson Strait, not through the York canyons. The York canyon floods evidently occurred in conjunction with blockage of Hudson Strait but could not have been the main egress of water and ice for any event of the size proposed, and the canyons are probably irrelevant in the discussion of Heinrich mechanisms. For the purposes of Johnson and Lauritzen's 116 ka event, the relevance of egress of ice is further complicated by the fact that while a large flux of initially grounded ice must be invoked to explain the inferred sea level rise, there is no Heinrich event in the marine record at this time.

There is also difficulty with the suggestion that a fall in lake level would initiate surges of ice terminating in the lake. While the removal of the supporting back stress of water would affect the force balance in floating ice and at the terminus [*Paterson*, 1980], the consequent loss of subglacial water pressure would suppress, rather than promote, upstream surge behavior [*Kamb et al.*, 1985; *Raymond*, 1987]. Surging of a glacier terminating in a lake is by no means a likely consequence of drainage of the lake. We propose that a general mechanism for rapid evacuation of ice and water from Hudson Strait and Hudson Bay may have more plausibly occurred as a consequence of a calving embayment rather than a flood/surge event. *Johnson and Lauritzen* [1995] refer to aspects of iceberg entrapment but do not pursue the implications. We suggest that ice grounded in eastern Hudson Strait from a Quebec/Labrador source (or ice grounded at that location for any reason) could have blocked the egress of icebergs delivered from calving termini in western Hudson Strait or surrounding Hudson Bay. The impounded icebergs, or sikkusaq, would provide a buttressing back stress once the open water is filled with ice (freezing of water around the icebergs speeds this process), and the reduced calving speed allows advance of the calving termini, creating a region of ice which is grounded but near flotation [*Andrews*, 1990; *Hughes*, 1992; *Meier and Post*, 1987; *Trabant et al.*, 1991]. When the blockage in eastern Hudson Strait is removed, possibly but not exclusively by a jökulhlaup, a calving embayment can develop and penetrate upstream quickly by the process of extensional thinning and ungrounding into the regions occupied by advance following the formation of the sikkusaq. This hypothesis allows for rapid discharge of large volumes of ice from Hudson Strait without necessitating a large initial ice volume in the interior or invoking jökulhlaups or surges, either of which require for their occurrence special conditions which are less likely to exist than those required to produce a calving embayment. Formation and removal of grounded ice by the sikkusaq/calving embayment process also preserves an attractive aspect of Johnson and Lauritzen's original hypothesis, namely, the rapid conversion of ice-covered areas to open water and vice versa. This aspect of either process provides a mechanism for rapid alterations in storm tracks and precipitation patterns. We note that neither Johnson and Lauritzen's hypotheses nor ours addresses the reasons why ice originating from Quebec/Labrador crossed Hudson Strait in the first place. For the purposes of our discussion of the Younger Dryas/DC-0 event, the field evidence that such an event did indeed occur is sufficiently strong that we can accept it as a given and focus on subsequent events. It is unresolved whether such cross-strait advances from Ungava Bay to Baffin Island occurred on any regular basis in the past. We note that no direct terrestrial or marine evidence exists for downstrait flow either.

3.5. Relation to Marine Event DC-0

Several features of DC-0 have particular relevance to the modeled pattern of ice advance and retreat described here. *Miller and Kaufman* [1990] were the first to identify the northward advance of ice from the Ungava platform across Hudson Strait to Frobisher Bay and the Baffin Shelf and, on the basis of the chronology available at the time, proposed that calving associated with advance to the Baffin Shelf was the trigger for the Younger Dryas cooling. Subsequently, however, improved dates shifted the chronology of both the terrestrial geology and the Younger Dryas. *Kaufman et al.* [1993] refined the cross-strait advance to a single maximum (Gold Cove) at 9.9-9.6 ka ^{14}C, associating it with the Preboreal cooling following the Younger Dryas

rather then with the Younger Dryas itself. Most recently, *Andrews et al.* [1995] show the Younger Dryas and DC-0 as being generally contemporaneous, initiating at ~11.0 ka ^{14}C and terminating prior to the Gold Cove maximum, although DC-0 does not show a sharp termination. In the present interpretation of events, Younger Dryas cooling could be the consequence of disruption of oceanic thermohaline circulation, especially in view of the evidence of iceberg discharge provided in DC-0, but the terrestrial evidence of delivery of ice from land to ocean appears to come too late to match DC-0.

Our model shows several results pertinent to this problem. First, advance of ice takes approximately 1.0 to 1.4 kyr to reach Gold Cove from its initial position on the Ungava platform. The Gold Cove advance was characterized by *Kaufman et al.* [1993] as very rapid in Frobisher Bay; the Gold Cove maximum can be seen here, however, as the culmination of a longer event which started from the Ungava platform at a time consistent with the onset of DC-0. Second, the maximum discharge of ice and runoff into Hudson Strait during advance (Figure 6) occurs early on as the advance enters the Eastern Basin. If the Younger Dryas cooling is partly or wholly a product of ice discharge from this event, the timing of input is not necessarily inconsistent. However, as detailed above, the magnitude of flux during advance is only one sixth of the lowest flux suggested by *Rahmstorf* [1995] as likely to affect thermohaline circulation. This model result is consistent with the suggestion of *Andrews et al.* [1991], based on isotopic indicators of surface salinity, that little freshening of waters occurred in Resolution Basin between 11 and 10 ka ^{14}C. Another feature of DC-0 difficult to reconcile with the Gold Cove advance is the decline in carbonate following 10.4 ka ^{14}C (e.g. *Andrews et al.*, [1995], Figure 5), still some 700 years prior to the arrival of ice at Gold Cove. Our model has grounded ice at the MIRI position at this time, and modeled fluxes decline at this point. We propose that DC-0 is the product of calving as ice crosses Hudson Strait, is initiated by events on land which start the northward advance from the Ungava platform, and is terminated by grounding of the advancing margin in the shallow waters of MIRI. The marine event DC-0 terminates at this point, but the advance of ice continues. Finally, DC-0 is most well defined in cores from Resolution Basin. This is consistent with our model results, which show an early peak discharge across the Resolution Island/Labrador sill into Hatton Basin but a later peak discharge of longer duration through the Resolution Island/Meta Incognita gap into Resolution Basin.

4. Discussion and Conclusions

1. The initial advance of ice from Quebec/Labrador was initiated by allowing sliding in Ungava Bay and regions to the north, and a stable position on MIRI was achieved over ~400 years. The speed and spatial pattern of advance was controlled by initial ice geometry and location of sliding. Initial ice dome height was the most significant controlling variable: A maximum ice thickness of at least 2000 m was required to drive advance because of the limit placed on flow by the frozen bed south of Ungava Bay. Total discharge to the ocean (calving plus runoff from marine based ice) reached a maximum value during advance of 0.0025 Sv as the advancing margin entered the deep Eastern Basin of Hudson Strait. The advance stabilized as ice encountered shallow water in the gaps between Labrador (Killineck Island), Resolution Island, and Meta Incognita Peninsula.

2. Advance from MIRI to Gold Cove was reproduced within the constraints of timing imposed by radiocarbon dates, but we could not obtain ice thicknesses at Hall Peninsula compatible with terrestrial evidence. The advance is driven by variations in local mass balance rather than upstream dynamics originating from the main dome, again as a consequence of isolation of the advancing lobe from the main dome by the frozen bed requirement under the main dome. Retreat from Gold Cove and subsequent evacuation of ice from Frobisher Bay and Hudson Strait is accomplished by a combination of drawdown of ice and rise in ELA. Discharge fluxes reach 0.011 Sv at the time of evacuation of ice from the Gold Cove maximum position. This value is close to 0.015 Sv suggested by *Rahmstorf* [1995] as sufficient to shut down Labrador Sea convection but occurs at the wrong time to act as a trigger for interruption of thermohaline circulation at the outset of the Younger Dryas. This discharge could have triggered the smaller Preboreal cooling event observed in the North Atlantic region [*Kaufman et al.*, 1993; *Lehman and Keigwin*, 1992; *Koc Karpuz and Jansen*, 1992; *Johnsen et al.*, 1992]. We conclude that ice discharge from Quebec/Labrador was not the sole source of a perturbation of North Atlantic ice and water discharge responsible for the postulated thermohaline shutdown at Younger Dryas time but may have acted in combination with overall runoff from the warming Arctic or other specific sources (e.g., Cumberland Sound [*Jennings et al.*, 1995]). We also find that *Miller and Kaufman*'s [1990] estimates of ice flux into the Labrador Sea are unrealistically high, both because of the constraint imposed by the ice volumes available in the main dome and the lobe extended north from Ungava Bay and because our modeling results suggest that cross-strait advance does not necessarily have to occur in conjunction with high rates of loss by calving at the mouth of Hudson Strait.

The model results presented here duplicate the geologically inferred spatial and temporal patterns of advance to Meta Incognita and Hall Peninsulas but do so with minimal ice thicknesses at Hall Peninsula and ice discharge less than that presently believed to be significant in terms of North Atlantic thermohaline circulation. Also, the model results are attainable only

by driving the free variables (initial ice thickness on Quebec/Labrador and mass balance) at extreme values. The very thick ice mass on Quebec/Labrador is unable to contribute much in terms of ice flux or dynamics to the advances since most of the mass is locked in place by the requirement of a frozen bed under the main dome south of Ungava Bay. We conclude that the frozen bed condition imposed by *Kleman et al.*'s [1994] interpretation of flow indicators on Quebec/Labrador is incompatible with what we regard as the more robust interpretation of flow indicators and ice thickness on Baffin Island and Hall Peninsula made by *Kaufman et al.* [1993]. The frozen bed condition forces us to push our free parameters (initial ice thickness and mass balance) to their limits to reproduce even a minimum-thickness advance to Gold Cove. We therefore shift our attention to an alternative suggested by *Clark et al.* [1996] which presents geomorphic evidence indicating sliding over a broad region south of Ungava Bay. We anticipate that more extensive basal sliding south of Ungava Bay will allow advance across Hudson Strait and beyond without requiring such extreme forcing through initial thickness and mass balance.

Acknowledgments. This work was supported by NSF grant EAR-9510063 and DOE grant DE- FGO3-93ER61689. We thank J.T. Andrews, J. Fastook, T.J. Hughes, B. MacLean, and G. H. Miller for thoughtful reviews and comments.

References

Alley, R.B., et al., Abrupt increase in Greenland snow accumulation at the end of the Younger Dryas event, *Nature, 362*, 527-529, 1993.

Andrews, J.T., Fiord to deep sea sediment transfers along the north-eastern Canadian continental margin: Models and data, *Geogr. Phys. Quat., 44(1)*, 55-70, 1990.

Andrews, J.T., L.W. Evans, K.M. Williams, W.M. Briggs, A.J.T. Jull, H. Erlenkeuser, and I. Hardy, Cryosphere/ocean interactions at the margin of the Laurentide Ice Sheet during the Younger Dryas chron: SE Baffin shelf, Northwest Territories, *Paleoceanography, 5*, 921-935, 1990.

Andrews, J.T., H. Erlenkeuser, L. Evans, W. Briggs, and A.J.T. Jull, Meltwater and deglaciation SE Baffin Shelf (NE margin Laurentide Ice Sheet) between 13.5 and 7 ka: From O and C stable isotopic data, *Paleoceanography, 6*, 621-637, 1991.

Andrews, J.T., A.E. Jennings, M. Kerwin, M. Kirby, W. Manley, G.H. Miller, G. Bond, and B. MacLean. A Heinrich-like event, H-0 (DC-0): Source(s) for detrital carbonate in the North Atlantic during the Younger Dryas chronozone, *Paleoceanography, 10*, 943-952, 1995.

Bard, E., M. Arnold, J. Mangerud, M. Paterne, L. Labeyrie, J. Duprat, M.-A. Melieres, E. Sonstegaard, and J.-C. Duplessy, The North Atlantic atmosphere-sea surface ^{14}C gradient during the Younger Dryas climatic event. *Earth Planet. Sci. Lett. 126*, 275-287. 1994.

Blake, W., End moraines and deglaciation chronology in northern Canada with special reference to southern Baffin Island, *Pap. Geol. Sur. Can., 66-26*, 31 pp., 1966.

Broecker, W.S., Massive iceberg discharges as triggers for global climate change, *Nature, 372*, 421-424, 1994.

Budd, W.F., Ice flow over bedrock perturbations, *J. Glaciol. 9(55)*, 29-48, 1970.

Clark, C.D., J.K. Knight, and J.T. Gray, Reconstructing ice dynamic scenarios for the Ungava sector of the Laurentide Ice Sheet. paper presented at the *26th Annual Arctic Workshop*, Inst. of Arct. and Alp. Res., Univ. of Colo., Boulder, March 14-16, 1996.

Dowdeswell, J.A., M.A. Maslin, J.T. Andrews, and I.N. McCave, Iceberg production, debris rafting, and extent and thickness of Heinrich layers (H-1, H-2) in North Atlantic sediments, *Geology, 23*, 301-304, 1995.

Edwards, R.L., Paleotopography of glacial-age ice sheets, *Science, 267*, 536, 1995.

Fastook, J., and J.E. Chapman, A map-plane finite element model: Three modeling experiments, *J. Glaciol., 35(119)*, 48-52, 1989.

Fastook, J., and W. Schmidt, Finite element analysis of calving from ice fronts, *Ann. Glaciol., 3*, 103-106, 1982.

Heinrich, H., Origin and consequences of cyclic rafting in the northeast Atlantic Ocean during the past 130,000 years, *Quat. Res., 29*, 142-152. 1988.

Hughes, T.J., Theoretical calving rates from glaciers along ice walls grounded in water of variable depths, *J. Glaciol., 38(129)*, 282-294, 1992.

International Association of Hydrological Sciences and United Nations Environmental Program (IAHS/UNEP), *Fluctuations of Glaciers, 1980-1985*, Edited by W. Haeberli and M. Hoelzle, World Glacier Monit. Serv., Zurich, 1988.

IAHS/UNEP, *Fluctuations of Glaciers, 1985-90*, Edited by W. Haeberli and M. Hoelzle, World Glacier Monit. Serv., Zurich, 1993.

Jennings, A. E., K. Tedesco, J.T. Andrews and M.E. Kirby, Shelf erosion and glacial ice proximity in the Labrador Sea during and after Heinrich events (H-3 or 4 to H-0) as shown by foraminifera, in *Late Quaternary Paleoceanography of North Atlantic Margins*, edited by J.T. Andrews, W. Austin, H. Bergsten, and A.E. Jennings, pp. 29-50, Geol. Soc. of London, 1995.

Johnsen, S.J., H.B. Clausen, W. Dansgaard, K. Fuhrer, N. Gundestrup, C.U. Hammer, P. Iversen, J. Jouzel, B. Stauffer, and J.P. Steffensen, Irregular glacier interstadials recorded in a new Greenland ice core, *Nature, 359*, 311-329, 1992.

Johnson, R.G., and S.-E. Lauritzen, Hudson Bay-Hudson Strait jökulhlaups and Heinrich events: A hypothesis, *Palaeogeogr., Palaeoclimatol., Palaeoecol., 177*, 123-137, 1995.

Kamb, B., and K.A. Echelmeyer. Stress-gradient coupling in glacier flow, I, Longitudinal averaging of the influence of ice thickness and surface slope. *J. Glaciol., 32(111)*, 267-284, 1986.

Kamb, B., C.F. Raymond, W.D. Harrison, H. Engelhardt, K.A. Echelmeyer, N. Humphrey, M.M. Brugman, and T. Pfeffer, Glacier surge mechanism: 1982-1983 surge of Variegated Glacier, Alaska, *Science, 227*, 469-479, 1985.

Kaufman, D.S., G.H. Miller, J.A. Stravers, and J.T. Andrews. An abrupt early Holocene (9.9-9.6 kyr P) ice stream advance at the mouth of Hudson Strait, Arctic Canada, *Geology, 21*, 1063-1066, 1993.

Kleman, J., I. Borgstrom, and C. Hattestrand, Evidence for a relict glacial landscape in Quebec-Labrador. *Palaeogeogr., Palaeoclimatol., Palaeoecol., 111*, 217-228, 1994.

Koc Karpuz, N.K., and E. Jansen, A high-resolution diatom record of the last deglaciation from the SE Norwegian Sea: Documentation of rapid climatic changes, *Paleoceanography, 7*, 499-520, 1992.

Krenke, A.N., and V.G. Chodakov, On the relationship between glacier melt and air temperature (in Russian with English summary), *Mater. Glaziol. Issl., 12*, 155-163, 1966.

Lauriol, B., and J.T. Grey, The decay and disappearance of the Late Wisconsin ice sheet in the Ungava Peninsula, northern Quebec, Canada, *Arct. Alp. Res., 19*, 109-126, 1987.

Lehman, S., and L. Keigwin, Sudden changes in North Atlantic circulation during the last deglaciation, *Nature, 356*, 757-762, 1992.

MacAyeal, D.R., Binge/purge oscillations of the Laurentide Ice Sheet as a cause of the North Atlantic's Heinrich events, *Paleoceanography, 8*, 775-784, 1993.

Manabe, S., and R. J. Stouffer, Simulation of abrupt climate change induced by freshwater input to the North Atlantic Ocean, *Nature, 378*, 165-167, 1995.

Manley, W., Late-glacial record of ice sheet/ocean interactions, Hudson Strait and southern Baffin Island, eastern Canadian Arctic, Ph.D. thesis, Dep. of Geolog. Sci., Univ. of Colo., Boulder, 1995.

Manley, W., B. MacLean, M.W. Kerwin, and J.T. Andrews, Magnetic susceptibility as a Quaternary correlation tool: Examples from Hudson Strait sediment cores, eastern Canadian Arctic, *Pap. Geol. Surv. Can., 93-1D*, 137-145, 1993.

Meier, M.F., and A. Post, Fast tidewater glaciers, *J. Geophys. Res., 92*, 9051-9058, 1987.

Miller, G.H., and D. Kaufman, Rapid fluctuations of the Laurentide Ice Sheet at the mouth of Hudson Strait: New evidence for ocean/ice-sheet interactions as a control on the Younger Dryas, *Paleoceanography, 5*, 907-919, 1990.

Miller, G.H., P.J. Hearty, and J.A. Stravers, Ice sheet dynamics and glacial history of southeasternmost Baffin Island and outermost Hudson Strait, *Quat. Res., 30*, 116-136, 1988.

National Oceanic and Atmospheric Administration, Digital relief of the surface of the earth, *Data Announce. 88-MGG-02*, Nat. Geophys. Data Cent., Boulder, Colo., 1988.

Ohmura, A., ETH Greenland Ice Sheet Program: An overview, Mass balance and related topics of the Greenland Ice Sheet, edited by N. Reeh and H. Oerter, *Open File Ser. 93/5*, Eidg. Tech. Hochsch., Zurich, 1993.

Paterson, W.S.B., Ice sheets and ice shelves, in *Dynamics of Snow and Ice Masses*, edited by S.C. Colbeck, pp. 1-78, Academic, San Diego, Calif., 1980.

Paterson, W.S.B., *The Physics of Glaciers*, 3rd ed., Elsevier, New York, 1994.

Peltier, W. R., Ice-age paleotopography, *Science, 265*, 195-201, 1994.

Rahmstorf, S., Bifurcations of the Atlantic thermohaline circulation in response to changes in the hydrological cycle, *Nature, 378*, 145-149, 1995.

Raup, B.H., Implementation of longitudinal stress coupling into a map-plane finite-element glacier flow model, M.A. thesis, Dep. of Geol. Sci., Univ. of Colo., Boulder, 1995.

Raymond, C.F., How do glaciers surge? A review, *J. Geophys. Res., 92*, 9121-9134, 1987.

Reeh, N., On the calving of ice from floating glaciers and ice shelves. *J. Glaciol., 7(50)*, 215-232, 1968.

Sassolas, C., W. T. Pfeffer, and B. Amadei, Stress interaction between multiple crevasses in glacier ice, *Cold Reg. Res. Eng., 24(2)*, 107-116, 1996.

Stravers, J. A., G.H. Miller, and D.S. Kaufman, Late glacial ice margins and deglacial chronology for southeastern Baffin Island and Hudson Strait, eastern Canadian Arctic, *Can. J. Earth Sci., 29*, 1000-1017, 1992.

Trabant, D.C., R.M. Krimmel, and A. Post, A preliminary forecast of the advance of Hubbard Glacier and its influence on Russell Fjord, Alaska, *U.S. Geol. Surv. Water Resour. Invest. Rep., 90-4172*, 34 pp, 1991.

M. Dyurgerov, and C. Sassolas, Institute of Arctic and Alpine Research, University of Colorado, Boulder, CO 80309. (e-mail:dyurg@tintin.colorado.edu; sassolas@tintin.colorado.edu)

A. Jennings, M. Kaplan, W. Manley, W. T. Pfeffer, Institute of Arctic and Alpine Research and Department of Geological Sciences, University of Colorado, Boulder, CO 80309. (e-mail: jenninga@spot.colorado.edu; kaplanm@ucsu.colorado.edu; manleyw@ucsu.colorado.edu; pfeffer@tintin.colorado.edu)

J. Dwyer, Department of Mechanical Engineering, University of New Hampshire, Durham, NH 03824. (e-mail: dwyer@mech2.unh.edu)

B. Raup, U. S. Geological Survey, Flagstaff, AZ, 86001. (e-mail: braup@flagmail.wr.usgs.gov)

(Received June 26, 1996; revised October 1, 1996; accepted October 8, 1996.)